Radiation Functionalisation of Thermal and Mechanical Properties of Polyethylene Composites with Multi-Walled Carbon Nanotube

Tatiana Pinchuk-Rugal
Taras Shevchenko National University of Kyiv
Andrii Misiura
Taras Shevchenko National University of Kyiv
Oksana Dmytrenko
Taras Shevchenko National University of Kyiv
Mykola Kulish
Taras Shevchenko National University of Kyiv
Andriy Momot
Taras Shevchenko National University of Kyiv
Olena Pavlenko
Taras Shevchenko National University of Kyiv
Maksim Alieksandrov
mrmarafon@gmail.com

V.E. Lashkaryov Institute of Semiconductor Physics of NAS of Ukraine
Oleksandr Kolomys
V.E. Lashkaryov Institute of Semiconductor Physics of NAS of Ukraine
Oleksii Melnychenko
SE “RADMA”, L. V. Pisarzhevsky Institute of Physical Chemistry of NAS of Ukraine
Yurii Onanko
Institute of Water Problems and Land Reclamation of the National Academy of Agrarian Sciences of Ukraine
Yevgen Mamunya
E.O. Paton Electric Welding Institute
Andrii Pylypenko
Institute of Macromolecular Chemistry of NAS of Ukraine

Research Article

Keywords: low-density polyethylene, electron irradiation, thermomechanical analysis, deformation, Raman spectroscopy, quantum chemical modelling

Posted Date: January 29th, 2026

DOI: https://doi.org/10.21203/rs.3.rs-8617859/v1

Additional Declarations: No competing interests reported.

Version of Record: A version of this preprint was published at Applied Composite Materials on July 7th, 2026. See the published version at https://doi.org/10.1007/s10443-026-10501-1.

Abstract

This study investigates radiation-functionalised low-density polyethylene (LDPE) nanocomposites containing multi-walled carbon nanotubes (MWCNTs) at absorbed doses ranging from 0.1 to 4.72 MGy. The thermophysical and mechanical properties, as well as the Raman spectra, of these composites were studied. An increase in the absorbed dose of electron irradiation, from 0.05 to 4.72 MGy, resulted in complex transformations of the intramolecular structure, due to the mechanochemical effect of macrochain destruction and cross-linking in crystalline and amorphous regions. Quantum chemical calculations were performed to optimise the geometry, infrared absorption spectra, combinational scattering, charge distribution, molecular orbital shapes, and localisation of energy levels within the electron forbidden zone. The electron transition configurations for the PE chain (C_9H_{20}) were also optimised. It was established that the C_9H_{20} molecule is linear with a trans conformation. Single bonds between carbon and hydrogen atoms form σ-type molecular orbitals. The frequencies of the calculated vibrational spectra best agree in the range of deformation vibrations.

1. Introduction

The carbon-chain polyethylene (PE) is widely used in a variety of technological industries. Various fillers, particularly carbon nanotubes (CNTs), are used to enhance the physical and mechanical properties of this polymer. This enables the properties of polyethylene to be varied over a wide range [1]. Due to the high electrical conductivity and mechanical properties of CNTs, significant electrical conductivity and improved mechanical characteristics can be achieved in PE composites [2]. The modification of the physical and mechanical properties of polymer composites depends significantly on the concentration of carbon nanotubes, their distribution in the polymer matrix and the manufacturing and processing methods. The interaction between the polymer component of the composite and the filler particles is equally important.

The interaction between the components of a polymer composite determines its electrical [3, 4], dielectric [5, 6] and mechanical properties. Many scientific studies in this field aim to investigate the interaction processes between the polymer matrix and the filler, the methods of influencing and improving this interaction, and the processes occurring at the interface, i.e. the contact boundary between the polymer and the filler particle. Another factor that can significantly affect the properties of both the polymer matrix and the composite is radiation functionalisation, which promotes the formation of free radicals and the cross-linking of polyethylene (PE).

A developed defect structure forms in polymers and their composites during synthesis and processing, or because of radiation damage. These defects can take various forms, including damage to the intramolecular structure and its supramolecular organisation. Among other defects, polyene defects are stable in carbon-chain polymers due to the action of ionising radiation. These defects can affect the physicochemical properties of polymers and their composites, including the modification of vibrational spectra [7–11].

This study aims to establish how interphase interaction influences the physical-mechanical, thermomechanical and oscillatory properties of radiation-functionalised polyethylene-MWCNT polymer composites.

2. Materials and methods

2.1. Sample preparation

A series of polyethylene samples and nanocomposites based on low-density polyethylene (PE) powder (type 168-03-070) were produced and filled with MWCNT. The nanotubes, which were produced by NANOCYL (Sambreville, Belgium), had a diameter of d = 9.5 nm and a length of l = 1.3 μm, and were selected as electrically conductive fillers. First, the PE powder was thoroughly mechanically mixed with the corresponding concentration of MWCNTs (1.0 and 2.0 vol.%) by grinding in a porcelain mortar. This resulted in the filler particles covering the surface of significantly larger polymer powder particles. Next, the mixture of polymer and MWCNT powders was placed in a steel mould, heated to 170°C, hot-compacted at 25 MPa, and cooled gradually to room temperature at a rate of 15°C/min. Using the hot compaction method and two different moulds, samples in shape of discs with a diameter of 30 mm and a thickness of ~ 1.5 mm and rectangular films with a thickness of ~ 250 μm were obtained.

2.2. Research methods

Thermomechanical studies were carried out on a Q400 EM thermomechanical analyser (TA Instruments, USA) in penetration mode. The samples were studied in a temperature range from 20 to 250°C at a heating rate of 10°C/min, under a constant load of 0.5 MPa.

The melting and crystallization behavior PE-MWCNT composites was studied using a differential scanning calorimeter (TA Instruments DSC Q2000, USA). The experiment was performed from room temperature up to 160 ^{o}C at a rate of 20 ^{o}C/min. After melting, the samples were held in the DSC chamber for 1 min before being cooled to room temperature at a rate of 20 ^{o}C/min. Then the sample was heated using the same method as the first cycle. From the second cycle of DSC studying, the crystallization temperature (T_c) and the crystallization enthalpy (H_c) were determined in accordance with the ISO 11357-3 standard.

The mechanical properties of pure polymer and composite films were studied using a uniaxial tensile test on a tensile testing machine (Shimadzu AGS-10kNX, Japan). The tensile speed was kept constant at 10 mm/min throughout the experiment, in accordance with ISO 527-3.

Raman spectra were studied using a Horiba Jobin Yvon T64000 triple spectrometer with an Ar-Kr ion laser with a wavelength of 514.5 nm. To excite the photoluminescence spectra, continuous He-Cd laser lines with a wavelength of 325 nm were used with the T 64000 micro-Raman spectrometer. The instrumental error of the device is 0.015 cm^{-1}.

The radiation exposure of the composites was carried out using an ILU-6 linear electron accelerator. The electron energy was E_e = 1.8 MeV. The selected absorbed doses were: 0.0, 0.05, 0.1, 0.2, 0.3, 0.5, 0.7, 2.0 and 4.72 MGy. The temperature of the samples during irradiation did not exceed 333 K.

Quantum chemical modelling of the PE chain was performed using the Gaussian 09 software package and the density functional theory (DFT) method with the B3LYP hybrid functional and 6-31G(d) basis set.

3. Results and discussion

3.1 Thermophysical studys

The thermophysical parameters of polymers and their composites are quite sensitive to the type, concentration of the filler and its structural organisation in the polymer matrix volume. It is particularly important in the context of considering the influence of interphase interaction on the characteristics of composites, since it determines the amount of filler that is in direct contact with the polymer [12]. Another important factor influencing the thermophysical parameters of a polymer material, including the interaction between its phases, is radiation exposure, which for a polyethylene matrix can result in the cross-linking of polymer chains or their destruction, depending on the absorbed dose [13].

The melting temperature of PE and its composites was determined based on the temperature dependence of the heat flow obtained using the DSC method. The degree of crystallinity of the studied samples was then calculated according to Eq. (1):

$$X_c\,(\%) = \frac{\Delta\, H_m}{\Delta\, H_m^o \cdot\, (1-\phi\,)} \cdot\, 100$$

1

where ΔH_m (J/g) is the melting enthalpy obtained from second heating DSC cycle of the sample, φ is the mass fraction of the MWCNT, and the ΔH_{0m} is the melting enthalpy of 100% crystalline PE (theoretical value of 293 J/g) [14].

Figure 1 shows a diagram demonstrating the melting point temperature (T_m) for unfilled PE and composites with a volume content of 1.0 vol.% MWCNT and 2.0 vol.% MWCNT depending on the absorbed dose.

As shown in Fig. 1, adding filler to the polymer matrix and increasing its concentration leads to an increase in the polymer material melting temperature (at 0 MGy): from 109.3°C for neat PE to 111.1°C for a composite with 1.0 vol.% MWCNT, and up to 112.2°C for 2.0 vol.%. This increase in melting temperature occurs because the filler particles restrict the thermal motion of the PE macromolecule chains and therefore require more thermal energy to become disordered during melting.

When neat PE is irradiated with a gradually increasing absorbed dose, a gradual decrease in the melting point to 103.5°C is observed at an absorbed dose of 0.5 MGy. For PE-MWCNT composites, a sharp decrease in T_m to 106.5°C and 107.1°C is observed at an absorbed dose of 0.1 MGy for 1.0 vol.% and 2.0 vol.% MWCNT, respectively. When the absorbed dose is increased to 0.3 MGy and 0.5 MGy, the T_m value decreases by approximately 2°C.

Adding filler and irradiating the composites also affects the degree of crystallinity of the polymer material (X_c%), as shown in Fig. 2.

According to Fig. 2, the degree of crystallinity of pure PE is 35.7%, and when it is filled with MWCNT, X_c decreases slightly to 35.4% for 1.0 vol.% MWCNT and 35.0% for 2.0 vol.% MWCNT. Similar behaviour is described in works [15, 16], where the degree of crystallinity of PE-based composites slightly decreases with the introduction of nanotubes. In the present study, the method of manufacturing the samples by hot compaction of a mechanical mixture of polymer and filler powders resulted in a specific arrangement of the filler within the polymer matrix volume, known as a segregated distribution [17]. Unlike the random (statistical) distribution type, in the segregated distribution type, the filler particles are localised in the area between large polymer particles rather than being distributed throughout the entire polymer matrix volume. Consequently, the contact area between the composite phases (polymer and filler) is significantly reduced, as is the influence of the filler surface on the crystal nucleation processes. Additionally, adding filler to the polymer matrix, particularly in significant quantities, increases the melt viscosity, which negatively affects the nucleation process. Together, these two factors lead to a slight decrease in the degree of crystallinity when MWCNTs are added to the PE matrix. Irradiation of the studied composites leads to a gradual decrease in the degree of crystallinity with an increase in the absorbed dose. Thus, at an absorbed dose of 0.5 MGy, X_c(PE) = 31.5%, X_c(PE-1.0% MWCNT) = 31.2%, X_c(PE-2.0% MWCNT) = 30.1%. This behaviour can usually be explained by the fact that irradiation, especially at high absorbed doses, causes cross-linking of polymer chains and even their destruction, which in turn negatively affects the value of X_c. Also, the crystalline regions formed during crystallisation will be more defective, i.e. imperfect, which should lead to a decrease in their melting point, as shown in Fig. 1.

The results of thermomechanical studies of PE and composites based on it filled with MWCNT are shown in Fig. 3.

Figure 3. Temperature dependence of PE deformation and composites based on it. Curves: 1, 2, 3 - absorbed dose – 0 MGy; 4, 5, 6 - absorbed dose – 0.1 MGy; 7, 8, 9 - absorbed dose – 0.3 MGy; 10, 11, 12 - absorbed dose – 0.5 MGy. Curves 1, 4, 7, 10 - PE; 2, 5, 8, 11 - PE-1.0 vol.% MWCNT; 3, 6, 9, 12 - PE-2.0 vol.% MWCNT.

Figure 3 shows the results of the thermomechanical analysis of irradiated PE composites with various absorbed doses. The TMA curves show the relative deformation values of the samples at a constant load of 0.5 MPa as a function of temperature. The relative deformation (ε) was calculated as follows:

$$\epsilon = (L - L_0)/L_0 \cdot 100\%$$

3

where: L_0 is the initial sample thickness and L is the current sample thickness.

In general, temperature-deformation curves show a slight increase in deformation in the positive direction. This corresponds to the thermal expansion of the pure polymer and the composites based on it. This is characteristic of both irradiated and unirradiated samples. Then, at $T > T_m$, a sharp increase in deformation is observed, which corresponds to the sample being pushed through under the action of an applied external load. This is followed by a region where the deformation remains almost unchanged. As can be seen in Fig. 3 for unirradiated samples (curves 1, 2 and 3), under a constant load creating a pressure of 0.5 MPa, the deformation of the samples reaches 100%. In contrast, for irradiated samples (curves 4–12), the deformation is significantly smaller and the sample pushes through slightly under an external pressure of 0.5 MPa, even at high temperatures. Based on the appearance of curves 4–12, it can be concluded that radiation-stimulated irradiation leads to a highly elastic state in PE and the disappearance of the transition to a highly fluid state [18].

As can be seen in Fig. 3, the sharp increase in sample deformation for unirradiated (0 MGy) and irradiated samples is spread over a wide range of temperatures. For curves 1–3, this interval is 111–119°C; for curves 4–12, it is 130–137°C. This behaviour of TMA dependencies could reflect PE chain breaking under irradiation, followed by cross-linking and the formation of a spatial network. This network increases the material's ability to resist external loads. Therefore, samples in which a spatial network of cross-linked PE chains has formed require more energy, i.e. higher temperatures, to alter the conformation of the macromolecular chains, thereby determining the deformation of the polymer material.

To better demonstrate the thermomechanical behaviour of samples at high temperatures ($T > T_m$), deformation values can be tracked at various temperatures, such as 150°C, 200°C and 250°C. Figure 4 shows one such cross-section, which illustrates the change in ε values from the absorbed dose. It depicts the deformation of neat polymer and composites with the addition of 1.0 vol.% and 2.0 vol.% MWCNT at different absorbed dose values and a temperature of 200°C.

A common characteristic of irradiated samples is that the deformation value decreases as the absorbed dose increases. For all series of irradiated samples, the dependence remains that the polymer composite with 2.0 vol.% MWCNT has the lowest ε value, while the unfilled polymer has the highest ε value. This demonstrates the influence of nanotubes on the material's ability to resist an applied load. Therefore, it can be concluded that the interaction between the composite's phases creates a reinforcing effect in the polymer matrix, thereby interfering with the thermal motion of PE chains. This filler effect can be attributed to the physical (adsorption) and chemical interaction between the two composite components at the filler-polymer interface. Depending on the activity of the fillers, the viscosity of

composites can increase as a result of adsorption interaction, even at low concentrations [19, 20]. When a load is applied to a polymer material with higher viscosity, its deformation will be less intense.

The curves in Fig. 3 also illustrate the change in ε with increasing temperature. For neat polyethylene (PE) and its composites with 1.0 and 2.0 vol.% MWCNT, irradiated with an absorbed dose of 0.1 MGy in the region $T > T_m$, an increase in deformation is observed with increasing temperature. However, when the absorbed dose increases to 0.3 MGy and 0.5 MGy, the trend reverses; at higher temperatures, the deformation value is smaller. This is particularly evident in curves 10, 11 and 12 in Fig. 3, which correspond to samples irradiated with an absorbed dose of 0.5 MGy. In the region $T > T_m$ for these curves, it can be said that thermal expansion of the samples is observed. Similar behaviour was observed for analogous systems in works [18, 21], which can be explained by the formation of a spatial network of cross-linked polymer chains, as discussed above.

3.2 Mechanical study

The next step was to investigate the mechanical characteristics of the composites, specifically their stress-strain relationship at room temperature, using tensile deformation. The values of the elastic modulus (*E*, MPa) and the percentage deformation at the point of sample rupture (*ε*, %) were determined from the obtained set of stress-strain curves, and are shown in Fig. 5 and Fig. 6, respectively.

As can be seen from Fig. 5, an increase in the content of MWCNTs in the composite leads to a rise in the material's modulus of elasticity. This effect is observed for both unirradiated samples (0 MGy) and for each absorbed dose during irradiation. Therefore, the assumption that the phases of the polymer composite interact and that the nanotubes have a reinforcing effect on the polymer matrix can be confirmed.

The elastic modulus values of samples that have been irradiated increase significantly compared to those of non-irradiated samples. This indicates the formation of a spatial network resulting from PE chain cross-linking under the action of irradiation. An increase in the value of *E* is observed when irradiated with an absorbed dose equivalent of 0.1 MGy or 0.3 MGy; a similar situation is described in [22]. However, for samples with an absorbed dose of 0.5 MGy, the elastic modulus decreases, though less than at 0.3 MGy and still greater than at 0.1 MGy. This can be explained by the fact that an absorbed dose equivalent of 0.5 MGy causes destructive effects on the molecular chain structure and the spatial network formed during cross-linking [23].

Figure 6 shows the deformation at break (*ε*, %) of PE and its composites at room temperature, as well as the effect of the absorbed dose on this value under irradiation.

As shown in Fig. 6, the data demonstrate a decrease in material deformation at break with an increase in the concentration of MWCNTs in the polyethylene matrix. This is because the filler acts as a stress concentrator, impairing the ability of PE chains to undergo conformational changes during deformation.

In other words, the nanotubes prevent some possible conformational transformations of the macromolecular chains when subjected to external loads, resulting in faster sample destruction.

For irradiated samples with absorbed dose equivalents of 0.1 MGy and 0.3 MGy, a decrease in deformation is observed as the absorbed dose increases. This indicates an increase in material fragility due to chain cross-linking and a decrease in mobility. Conversely, for samples with an absorbed dose of 0.5 MGy, an increase in ε is observed, demonstrating the superiority of the destructive effect of irradiation over its ability to form a spatial network of cross-linked chains. More precisely, at high doses of irradiation, the formed spatial network degrades. This allows certain conformational transformations of the chains to occur during deformation of the polymer composite material. This results in an increase in deformation at break.

3.3 Raman spectroscopy

As shown by the authors [24], for pure LDPE at low and intermediate absorbed doses of high-energy electron irradiation of 0.01–0.7 MGy, all vibrational modes characteristic of polyethylene [25, 26] are observed, with a change in background behaviour in the range near the overtone at 2730 cm^{-1}. At the highest absorbed doses (2.0-4.72 MGy), cross-linking and degradation processes lead to polyethylene destruction [27].

Figure 7 shows the Raman spectra of polyethylene containing 1.0 vol.% MWCNT in an unirradiated state and after receiving various doses of electron irradiation. This spectrum is clearly the result of the superposition of two spectra: the Raman spectra of carbon nanotubes and polyethylene. The Raman spectrum of the nanotubes exhibits noticeable bands at frequencies of 970, 1354, 1595 and 2709 cm^{-1}, corresponding to radial breathing modes, defects in the nanotubes, the fundamental tangential vibrational mode E_{2g} and the overtone of vibrations localised at defects, respectively. In the frequency range near 1064 and 1131 cm^{-1}, the bands belong to the valence vibrations of C–C stretching. Additionally, twisting modes $\varepsilon_t(CH_2)$ appear near 1295 cm^{-1}, bending modes $\delta(CH_2)$ appear near 1436 cm^{-1}, and valence stretching modes $\nu(CH_2)$ appear near 2853 and 2884 cm^{-1}. An intense band is also observed at 3081 cm^{-1}, which is not typically present in Raman spectra of polyethylene and nanotubes under normal conditions.

Electron irradiation with an absorbed dose of 0.05 MGy leads to the rearrangement of PE and nanotubes (see Fig. 7(b)). Not only does the intensity of the ν_s(C–C) peak decrease, but the value of the ν_{as}(C–C) band decreases too. The bands near 1067 and 1127 cm^{-1} become almost equal in intensity to the band near 1090 cm^{-1}, which is associated with macromolecules in a goose-foot conformation. At the same time, the positions of the bands at 1295, 1440 and 1461 cm^{-1}, which are characteristic of the orthorhombic phase of PE, are restored. Compared to the unirradiated sample, the G-band shifts significantly from 1595 cm^{-1} to 1585 cm^{-1}, which also indicates the formation of radiation defects in the nanotubes. It is also notable that the band at 3077 cm^{-1} is low in intensity.

At a higher absorbed dose of 0.2 MGy, radiation cross-linking plays a major role than destruction. The main difference in the Raman spectrum for this nanocomposite, compared to the sample irradiated with an absorbed dose of 0.05 MGy, is the appearance of a fairly intense band at 3079 cm^{-1}. It is obvious that this band is the result of the formation of unsaturated = C–H bonds under the action of irradiation. At this absorption dose, the main mechanism of macrochain cross-linking is the recombination of free radicals without the involvement and destruction of vinylene double bonds. Destruction plays a secondary role compared to cross-linking, which contributes to a decrease in the slighty degree of crystallinity.

As with a dose of 0.2 MGy, the Raman spectrum at the next absorbed dose of 0.7 MGy retains the main features characteristic of this nanocomposite (Fig. 7(d)). A very intense band is visible near 3078 cm^{-1}. Damage to the PE vibration bands persists. As with an absorbed dose of 0.7 MGy, the overall intensity of the Raman spectrum continues to decrease with an increase in the absorbed dose of electron irradiation to 2.0 MGy (Fig. 7(e)). Significant restructuring of the Raman spectrum occurs across all frequency ranges. Despite the preservation of the PE vibrational modes, the intensity, position and width of the bands change significantly. All valence vibration bands are preserved, with components at 2852, 2893 and 2930 cm^{-1}. The band corresponding to the double bond = C–H at 3080 cm^{-1} becomes wide and almost reaches the intensity of the valence vibration band. The D- and, in particular, the G- bands of nanotubes become much more complicated. Within the range of tangential vibrations, an intense component of the D'-band is present at 1604 cm^{-1}, alongside a less intense component at 1515 cm^{-1}. Thus, in the amorphous phase, the structure undergoes a complex restructuring process, which, as in the case of a sample irradiated with an absorbed dose of 0.7 MGy, involves the formation of a developed spatial network of cross-linked macrochains, as well as a high content of polyene sequences. Due to the creation of radiation damage and interlayer cross-links, irradiation significantly affects the structure of nanotubes and, consequently, their effectiveness as a filler.

As can be seen in Fig. 7(f), which shows the Raman spectrum of a PE nanocomposite containing 1.0 vol.% MWCNT after electron irradiation with an absorbed dose of 4.72 MGy, processes like those occurring in a nanocomposite irradiated with an absorbed dose of 2.0 MGy are taking place in the specified sample. Clearly, the created effective spatial lattice suppresses crystallisation processes within the amorphous phase. Conversely, intramolecular cross-linking in crystalline regions occurs at high absorption doses and leads to the amorphisation of these regions. It is possible that, at this absorption dose, the polyethylene structure is chemically destroyed. The presence of an intense band corresponding to unsaturated bonds indicates the accumulation of further polyene sequences in polyethylene. Thus, in a polyethylene nanocomposite containing 1.0 vol.% MWCNT, complex transformations of its structure occur at the intramolecular and intermolecular levels as the absorbed dose of electron irradiation increases from 0.05 to 4.72 MGy. This is due to a combination of mechanical and chemical effects resulting from the destruction and cross-linking of macromolecules in crystalline and amorphous regions, which are caused by ionising radiation. This is why interphase interaction plays a decisive role in polymer composites.

Figure 8 shows the Raman spectra of polyethylene containing 2.0 vol.% MWCNT in an unirradiated state and at various absorbed doses of electron irradiation. Like the nanocomposite with 1.0 vol.% MWCNT, the Raman spectra of the sample with 2.0 vol.% nanotubes appear similar in all states considered. They are characterised by a combination of Raman spectra from PE and the nanotubes. Scattering in the valence vibration range (v(C–C), δ(CH_2)) is significantly lower than the scattering intensity in the D- and G-bands of the nanotubes. At the same time, the intensity of the valence vibration bands (v(CH_2)) remains significant. In addition to the lines in the Raman spectrum of the unirradiated nanocomposite and the sample containing 1.0 vol.% MWCNT, an additional v(= CH) band appears at 3081 cm^{-1}. However, this disappears with an absorption dose of 0.05 MGy. Compared to the nanocomposite with 1.0 vol.% MWCNT, the mechanical and chemical damage to polyethylene caused by 2.0 vol.% nanotubes are more significant. This is evidenced by the absence of bands belonging to C–C valence vibrations at 1064 and 1131 cm^{-1} and bending deformation vibrations at 1463 cm^{-1} in the Raman spectrum. Significant shifts are also observed in the valence vibration bands, with the v(CH_2) band shifting from 2848 to 2855 cm^{-1} and the v(CH_2) band shifting from 2882 to 2893 cm^{-1}. Unlike the sample with 1.0 vol.% MWCNT, the intensity of the $v_s(CH_2)$ band at 2855 cm^{-1} exceeds that of the $v_{as}(CH_2)$ band at 2893 cm^{-1}.

These destruction mechanisms are primarily found in amorphous areas. In the Raman spectra, RDM bands are observed near 980 cm^{-1} and D* near 2706 cm^{-1}. The latter are quite intense due to the effective transfer of stresses from PE to nanotubes, indicating significant interaction between PE macromolecules and nanotubes. Electron irradiation of PE nanocomposites containing 2.0 vol.% of nanotubes and an absorbed dose of 0.05 MGy results in a significant rearrangement of the Raman spectra across different frequency ranges. Damage to the intramolecular and supramolecular structure continues. This is partly a consequence of ongoing destruction and partly due to the formation of a spatial network through ion-molecular and radiation cross-linking of unsaturated bonds. In the Raman spectrum of the nanocomposite with 2.0 vol.% nanotubes, the intensity of the v(= CH) band at 3079 cm^{-1} is low for the sample with 1.0 vol.% MWCNT. Interaction between the nanotubes and the PE macromolecules leads to broadening of the D- and G-bands and a significant increase in the intensity of the D*-band, which is sensitive to such interaction. This interaction may result from radiation cross-linking occurring not only between macromolecules, but also between them and the nanotubes. The degradation of macromolecules and the breakdown of the crystal structure occur via mechanisms like those in a nanocomposite containing 1.0 vol.% MWCNT.

An increase in the absorbed dose to 0.2 MGy continues to facilitate radiation cross-linking processes. At an absorbed dose of 0.2 MGy, the behaviour of the Raman spectrum resembles that at an absorbed dose of 0.05 MGy. A low-intensity broad band (v(= CH)) appears in the Raman spectrum at around 3081 cm^{-1}.

The bands corresponding to PE vibrations are strongly suppressed. The intensity of the $v_s(CH_2)$ band at around 2854 cm^{-1} increases sharply compared to the intensity of the $v_{as}(CH_2)$ band at around 2883 cm^{-1}. The latter band broadens due to the presence of Fermi resonance components with

macromolecules at 2897 and 2929 cm^{-1}. The intense D* overtone band near 2702 cm^{-1} is preserved. As the absorbed dose increases to 0.7 MGy, the Raman spectrum decreases sharply in the frequency ranges where the PE and MWCNT vibration bands are observed. Alongside the suppression of the intensity of all bands, there is significant broadening of the $\nu(CH_2)$ bands and a substantial shift in the position of the asymmetric valent vibrational mode band of the $\nu_{as}(CH_2)$ band to 2870 cm^{-1}.

The intensity of the ν(= CH) band at 3078 cm^{-1} exceeds that of the valence vibration bands of the $\nu(CH_2)$ group. The G band shifts significantly to 1583 cm^{-1}, while the intensity of the D' component near 1618 cm^{-1} increases sharply. The intensity of the D* overtone band approaches that of the $\nu(CH_2)$ bands. These changes to the Raman spectrum indicate that radiation cross-linking continues to promote intermolecular ordering. An absorbed dose of 2.0 MGy results in a significant rearrangement of the Raman spectra for both polyethylene and nanotubes. This indicates radical changes in the structure of the amorphous part, consisting not only of the formation of a spatial cross-linked network, but also of polyene sequence formation. The specified mechanisms of radiation-stimulated restructuring of polyethylene filled with nanotubes are manifested by the merging of the valence vibration $\nu(CH_2)$ and Fermi resonance bands, and a significant increase in the width and intensity of the ν(= CH) band of unsaturated C = C bonds.

At an absorbed dose of 4.72 MGy, radiation-stimulated structural rearrangement is accompanied by intramolecular cross-linking in crystallites, as well as the potential chemical breakdown of macromolecules (see Fig. 8(f)).

As can be seen, the $\nu_{as}(CH_2)$ band at 2893 cm^{-1} continues to shift towards higher frequencies. The integral intensity of the combined valence vibration band decreases. The intensity of the ν(= CH) band is significantly higher than that of the $\nu(CH_2)$ band. Therefore, despite the higher concentration of nanotubes in the nanocomposite containing 2.0 vol.% of MWCNTs, the mechanisms of radiation-stimulated rearrangement of the intramolecular and supramolecular structures are like those in the PE nanocomposite containing 1.0 vol.% of nanotubes.

3.4. Quantum chemical study

Quantum chemical optimisation of the polyethylene molecular chain containing nine links was also performed to study its molecular structure and electronic states. Figure 9 shows the optimised geometry and charge distribution of the C_9H_{20} polyethylene molecule.

The molecule is linear with a trans conformation. The optimised bond lengths along the chain are all identical, measuring 1.534 Å. The only exception is the C-C bond lengths of the terminal $–CH_3$ group, which are slightly shorter at 1.532 Å.

The uniform length and saturation of hydrocarbon bonds ensure an even distribution of charges on atoms (Fig. 9b). Consequently, the charges on the carbon atoms are identical, amounting to -0.25 e.u.

and 0.126 e.u. for the hydrogen atoms (excluding terminal groups). Due to the uniform distribution of charges along the polyethylene chain, the dipole moment is zero.

Figure 10 shows the distribution of electron energy levels and molecular orbital shapes for polyethylene. The strong nature of the σ-type molecular orbitals formed by single bonds between carbon and hydrogen atoms ensures their relatively high energies.

The vertical blue lines in Fig. 10 represent the wavelengths of electronic transitions, along with their respective oscillator strengths. Values for the most intense transitions are provided in Table 1.

Table 1
Wavelength and oscillator strengths of the most intense transitions in the optical spectrum of a nine-membered polyethylene molecule.

Wavelength (nm)	Oscillator strengths
116.26	0.1509
109.81	0.2301
107.21	0.4469
105.17,	0.4889
102.92	0.2275
101.4	0.2943

While the calculated and experimental spectra are qualitatively similar, the position of the absorption maximum differs significantly: 108.6 nm in the calculated spectrum and approximately 200 nm in the experimental spectrum. This is because the calculation was performed for a single polyethylene molecule; interaction with other molecules was not considered. Additionally, the polymer chain length used in the calculations (9 links) is significantly shorter than that of the polymer in the experimental samples.

3.5. Infrared and Raman spectroscopy modelling

Figure 11. Calculated IR absorption spectrum of the polyethylene molecule C9H20 (scale factor 0.9614).

The calculated infrared (IR) absorption spectrum contains bands of low frequency (714–872 cm^{-1} – CH_2 deformation rocking vibrations), mid-frequency (1078–1470 cm^{-1} – CH_2 twisting and bending deformation vibrations, respectively) and high-frequency (2900–2990 cm^{-1} – valence antisymmetric vibrations of methyl CH_3 groups).

Table 2 shows a comparison of the calculated and experimental frequencies of the IR spectrum for the LDPE molecule.

Table 2
Frequencies of calculated v_{calc} and experimental v_{exp} IR vibrational modes and types of vibrations for the C_9H_{20} molecule, corresponding to one monomeric link of LDPE.

v_{calc}, cm^{-1}	v_{exp}, cm^{-1} [24]	Type of oscillations
714	720	δ_r CH_2
872	880	$\delta_т$ CH_3
1301	1303	$\delta_т$ CH_2
1470	1460	$\delta_в$ CH_2
2909	2926	$v_{as}(CH_3)$
2959	2959	$v_{as}(CH_3)$
2988	~ 2970–3030	$v_{as}(CH_3)$

As can be seen, the calculated modes of vibration of the IR spectrum are in good agreement with the experimental data obtained by the authors in [24], with only minor frequency shifts.

Figure 12 shows the calculated Raman spectrum of the polyethylene molecule C_9H_{20}, the monomeric structure of which is shown in Fig. 9.

Intense bands appear in the frequency ranges 860–1460 cm^{-1} and 2500–3000 cm^{-1}.

Table 3 shows a comparison of the calculated and experimental frequencies of the LDPE molecule.

Table 3
Frequencies of calculated v_{calc} and experimental v_{exp} oscillatory modes and types of oscillations for the C_9H_{20} molecule, corresponding to one monomeric chain of LDPE.

v_{calc}, cm^{-1}	v_{exp}, cm^{-1} [24]	Type of oscillations
1032	1063	$v_{as}(C–C)(B_{2g})$
1118	1130	$v_s(C–C)(A_g+B_{1g})$
1290	1295	$\tau(CH_2)$(twisting CH_2, $B_{2g} + B_{3g}$)
1459	1416 + 1440 ≈ 1460	$\delta(CH_2)$(bending, B_{1g})
-	~ 2848	$v_s(CH_2)$ (A_g+B_{1g})
2890	2882	$v_{as}(CH_2)(A_g+B_{1g})$

As can be seen, the calculated frequencies of the different vibrational modes agree with the experimental results obtained by the authors in [24], to varying degrees. The best agreement is observed in the deformation vibration range of 1060–1460 cm^{-1}. Conversely, for high-frequency vibrational modes, there is less agreement between the calculated and experimental values of this molecule's frequencies.

5.Conclusions

The thermophysical, spectroscopic and mechanical properties of polyethylene (PE) and composites filled with multi-walled carbon nanotubes (MWCNTs) based on it are complex and depend on the absorbed dose. Irradiation of PE-based polymer composites has two effects: cross-linking forms a spatial network of polymer chains, and the material degrades at high doses of irradiation. Introducing a filler and cross-linking macromolecular chains significantly affects the conformational transformations of macromolecules, reflected in changes to the polymer material's properties.

1. An increase in the absorbed dose during irradiation leads to a decrease in the material's melting point and degree of crystallinity, due to the formation of a defective structure.
2. Thermomechanical studies have revealed a notable decrease in the deformation of irradiated PE-MWCNT composites. For a series of samples with an absorbed dose of 0.5 MGy, thermal expansion was observed at temperatures above 180°C in the region of highly elastic deformation.

3. The mechanical properties of PE-MWCNT composites, specifically the modulus of elasticity and deformation at break, exhibit non-monotonic behaviour. The elastic modulus increases with an increase in the absorbed dose during irradiation up to 0.3 MGy; however, for 0.5 MGy, it begins to decrease. Meanwhile, the deformation at break exhibits the opposite behaviour, which is associated with the degradation of the spatial network of cross-linked PE chains.
4. The calculated and experimental Raman spectra correlate best in the 1060–1460 cm^{-1} frequency range of deformation vibrations.
5. The presence of an intense band of Raman spectra for PE corresponding to double bonds = C–H at about 3081 cm^{-1} at different doses of electron irradiation absorption indicates the formation of π-conjugated polyene sequences. For PE nanocomposites with 1.0 and 2.0 vol.% MWCNT, the mechanisms of radiation-stimulated transformations of the intramolecular and supramolecular structure remain similar. They include: mechanochemical and radiation destruction of the crystalline phase, radiation cross-linking of macromolecules with the formation of π-conjugated polyene sequences of various lengths, and radiation damage to carbon nanotubes.
6. There is qualitative agreement between the bands of the main vibrations in the calculated IR and Raman spectra, with slight frequency shifts.

Declarations

CRediT authorship contribution statement

Tatiana Pinchuk-Rugal Writing – original draft; **Andrii Misiura** - Writing – original draft, Investigation; **Oksana Dmytrenko** - Writing – review and editing, Project administration; **Mykola Kulish** - Conceptualization, Supervision; **Andriy Momot** - Software, Visualization; **Olena Pavlenko** - Data curation, Validation; **Maksim Alieksandrov** - Investigation; **Oleksandr Kolomys** - Validation; **Oleksii Melnychenko** – Visualization; **Yurii Onanko** - Methodology; **Yevgen Mamunya** - Resources, Formal analysis; **Andrii Pylypenko** - Investigation.

Declaration of competing interest

The authors declare that they have no known competing financial interests or personal relationships that could have appeared to influence the work reported in this paper.

References

1. Harris, P.J.F.: Carbon nanotube composites. Int. Mater. Rev. **49**, 31–43 (2004). https://doi.org/10.1179/095066004225010505
2. Gorrasi, G., Di Lieto, R., Patimo, G., De Pasquale, S., Sorrentino, A.: Structure–property relationships on uniaxially oriented carbon nanotube/polyethylene composites. Polymer. **52**, 1124–1132 (2011). https://doi.org/10.1016/j.polymer.2011.01.008

3. Li, S., Yin, G., Chen, G., Li, J., Bai, S., Zhong, L., Zhang, Y., Lei, Q.: Short-term breakdown and long-term failure in nanodielectrics: a review. IEEE Trans. Dielectr. Electr. Insul. **17**, 1523–1535 (2010). https://doi.org/10.1109/tdei.2010.5595554
4. Lai, Y.-R., Yu, K.-F., Lin, Y.-H., Wu, J.-C., Lin, J.-J.: Observation of fluctuation-induced tunneling conduction in micrometer-sized tunnel junctions. AIP Adv. **2** (2012). https://doi.org/10.1063/1.4749251
5. Nan, C., Shen, Y., Ma, J.: Physical properties of composites near percolation. Annu. Rev. Mater. Sci. **40**, 131–151 (2010). https://doi.org/10.1146/annurev-matsci-070909-104529
6. Lewis, T.J.: Interfaces are the dominant feature of dielectrics at the nanometric level. IEEE Trans. Dielectr. Electr. Insul. **11**, 739–753 (2004). https://doi.org/10.1109/tdei.2004.1349779
7. Dintcheva, N.T., La Mantia, F.P., Malatesta, V.: Photo-oxidation behaviour of polyethylene/multi-wall carbon nanotube composite films. Polym. Degrad. Stab. **94**, 162–170 (2008). https://doi.org/10.1016/j.polymdegradstab.2008.11.012
8. Nychyporenko, O.S., Dmytrenko, O.P., Kulish, M.P., Pinchuk-Rugal, T.M., Grabowskiy, Y.Y., Zabolotniy, M.A., Strel'chuk, V.A., Nikolenko, A.S., Sementsov, Y.I., Mamunya, Y.P.: Radiation Technologies of Polymer Composites Properties Modification, in: NATO Science for Peace and Security Series. C, Environmental Security 69–77. (2014). https://doi.org/10.1007/978-94-017-9005-5_7
9. Kazimi, M.R., Faizal, C.K.M., Jamari, S.S., Shah, T.: Naqvi. Sulfonation of polyethylene improves functionality for fabricating technical textiles. Soc. Plast. Eng. (2014). 10.2417/spepro.005306
10. Sato, H., Shimoyama, M., Kamiya, T., Amari, T., Šašic, S., Ninomiya, T., Siesler, H.W., Ozaki, Y.: Raman spectra of high-density, low-density, and linear low-density polyethylene pellets and prediction of their physical properties by multivariate data analysis. J. Appl. Polym. Sci. **86**, 443–448 (2002). https://doi.org/10.1002/app.10999
11. Ferry, M., Ahn, Y., Dantec, F.L., Ngono, Y., Roma, G.: Combining experimental and theoretical tools to probe Radio-Oxidation products in polyethylene. Polymers. **15**, 1537 (2023). https://doi.org/10.3390/polym15061537
12. Alieksandrov, M., Misiura, A., Pinchuk-Rugal, T., Grabovskii, Y., Onanko, A., Dmytrenko, O., Kulish, M., Pavlenko, E., Busko, T., Pundyk, I., Gaponov, A., Taras, A.L.: Structural features of polymer nanocomposite LDPE–MWCNT in the percolation transition region of electrical conductivity. Nanosistemi Nanomateriali Nanotehnologii. **18**, 299–310 (2020). https://doi.org/10.15407/nnn.18.02.299
13. Zaharescu, T., Mariş, M.: Irradiation Effects in Polymer Composites for Their Conversion into Hybrids. J. Compos. Sci. **6**, 109–136 (2022). https://doi.org/10.3390/jcs6040109
14. Poh, L., Wu, Q., Chen, Y., Narimissa, E.: Characterization of industrial low-density polyethylene: a thermal, dynamic mechanical, and rheological investigation. Rheol. Acta. **61**, 701–720 (2022). https://doi.org/10.1007/s00397-022-01360-1
15. Konstantopoulos, G., Maroulas, P., Dragatogiannis, D.A., Koutsoumpis, S., Kyritsis, A., Charitidis, C.A.: The effect of interfacial resistance and crystallinity on heat transfer mechanism in carbon nanotube

reinforced polyethylene. Mater. Design. **199**, 109420 (2020). https://doi.org/10.1016/j.matdes.2020.109420

16. Kodjie, S.L., Li, L., Li, B., Cai, W., Li, C.Y., Keating, M.: Morphology and crystallization behavior of HDPE/CNT nanocomposite. J. Macromolecular Sci. Part. B. **45**, 231–245 (2006). https://doi.org/10.1080/00222340500522299
17. Misiura, A.I., Maruzhenko, O.V., Mamunya, Y.P., Kulish, M.P.: Influence of the type of filler distribution on the electrical and thermal conductivity of metal-filled polymer composite. Funct. Mater. **27**, 500–507 (2020). https://doi.org/10.15407/fm27.03.500
18. Nychyporenko, O.S., Dmytrenko, O.P., Kylish, M.P., Pinchuk-Rugal', T.M., Grabovsky, Y.Y., Zabolotny, M.A., Mamunya, Y.P., Levchenko, V.V., Shlapatska, V.V., Strelchuk, V.V., Tkach, V.M.: Radiation-stimulated alteration of electrical conductivity of polyethylene nanocomposites with carbon nanotubes. Probl. At. Sci. Technol. (PAST). **2**, 99–106 (2016)
19. McNally, T., Pötschke, P., Halley, P., Murphy, M., Martin, D., Bell, S.E.J., Brennan, G.P., Bein, D., Lemoine, P., Quinn, J.P.: Polyethylene multiwalled carbon nanotube composites. Polymer. **46**, 8222–8232 (2005). https://doi.org/10.1016/j.polymer.2005.06.094
20. Xiao, K., Zhang, L., Zarudi, I.: Mechanical and rheological properties of carbon nanotube-reinforced polyethylene composites. Compos. Sci. Technol. **67**, 177–182 (2006). https://doi.org/10.1016/j.compscitech.2006.07.027
21. Nychyporenko, O.S., Pinchuk-Rugal', T.M., Kovalyova, D.O., Dmytrenko, O.P., Kulish, M.P., Mamunya, Y.P., Levchenko, V.V., Shlapatska, V.V.: Radiation modification of polyethylene nanocomposites with multiwalled carbon nanotubes. Probl. At. Sci. Technol. (PAST). **4**, 44–48 (2014)
22. Mészáros, L., Kara, Y., Fekete, T., Molnár, K.: Development of self-reinforced low-density polyethylene using γ-irradiation cross-linked polyethylene fibres. Radiat. Phys. Chem. **170**, 108655 (2019). https://doi.org/10.1016/j.radphyschem.2019.108655
23. Smirnov, Y.N., Allayarov, S.R., Lesnichaya, V.A., Ol'khov, Y.A., Belov, G.P., Dixon, D.A.: The effect of gamma-radiation on polymer composites based on thermoplastic matrices. High Energy Chem. **43**, 449–455 (2009). https://doi.org/10.1134/s001814390906006x
24. Nychyporenko, O.S., Dmytrenko, O.P., Kulish, M.P., Pinchuk-Rugal, T.M., Grabovskyj, Y.E., Zabolotnyj, M.A., Bulavin, L.A., Mamunya, E.P., Levchenko, V.V., Strelchuk, V.V., Kutsaj, O.M., Shlapatska, V.V.: Radiation-induced structure transformation and vibrational spectra of polyethylene. Nuclear Phys. At. Energy. **16**, 367–373 (2015). https://doi.org/10.15407/jnpae2015.04.367
25. Furukawa, T., Sato, H., Kita, Y., Matsukawa, K., Yamaguchi, H., Ochiai, S., Siesler, H.W., Ozaki, Y.: Molecular structure, crystallinity and morphology of Polyethylene/Polypropylene blends studied by Raman Mapping, scanning electron microscopy, wide angle X-Ray diffraction, and differential scanning calorimetry. Polym. J. **38**, 1127–1136 (2006). https://doi.org/10.1295/polymj.pj2006056
26. Kida, T., Hiejima, Y., Nitta, K.-H.: Raman Spectroscopic Study of High-density Polyethylene during Tensile Deformation. Int. J. Experimental Spectroscopic Techniques. **1**, 1–6 (2016). https://doi.org/10.35840/2631-505x/8501

27. Perraud, S., Vallat, M., Kuczynski, J.: Radiation Crosslinking of Poly(ethylene-co-octene) with Electron Beam Radiation. Macromol. Mater. Eng. **288**, 117–123 (2003). https://doi.org/10.1002/mame.200390004

Figures

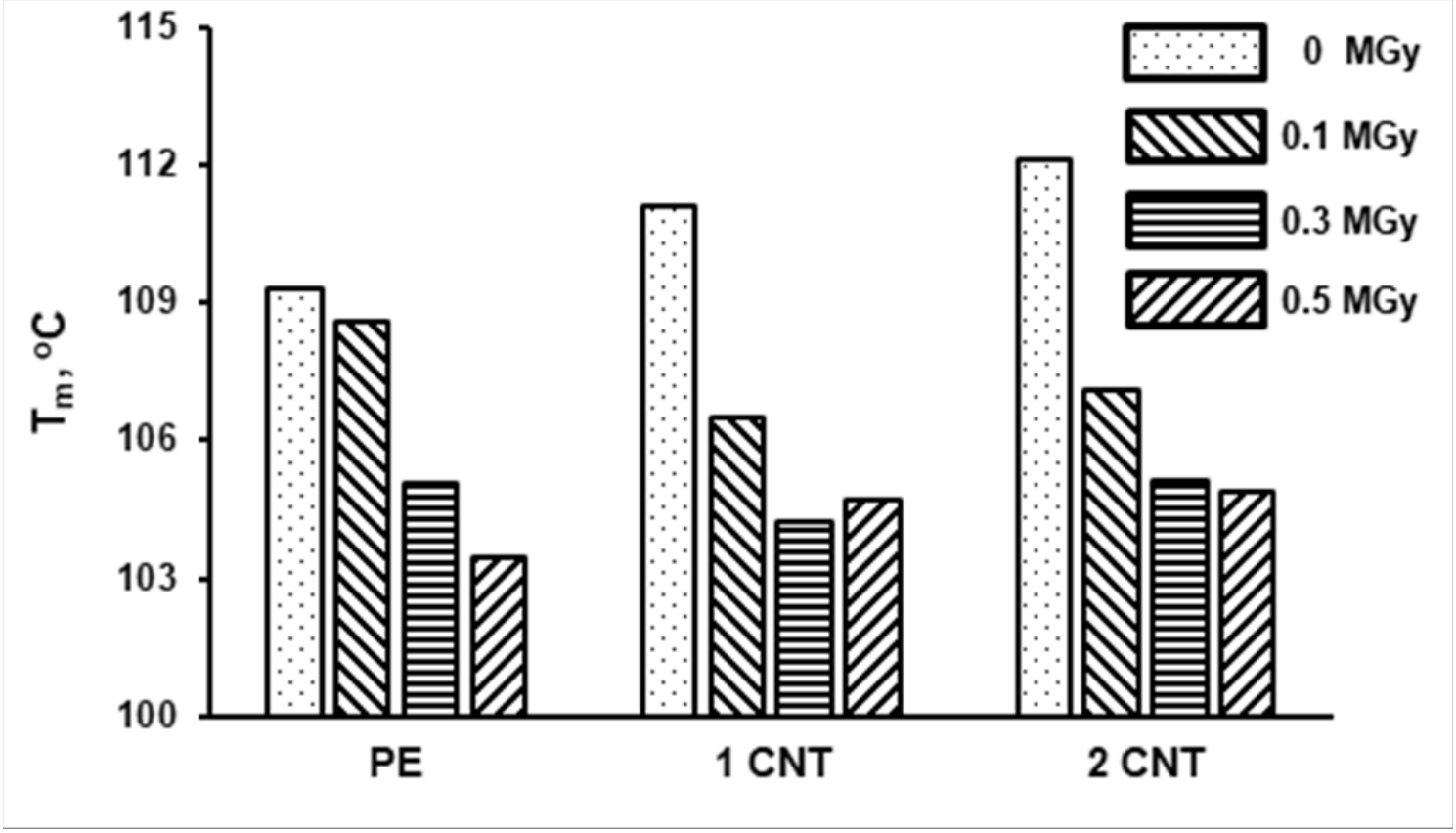

Figure 1

Melting temperature of PE and its composites at different absorbed radiation doses.

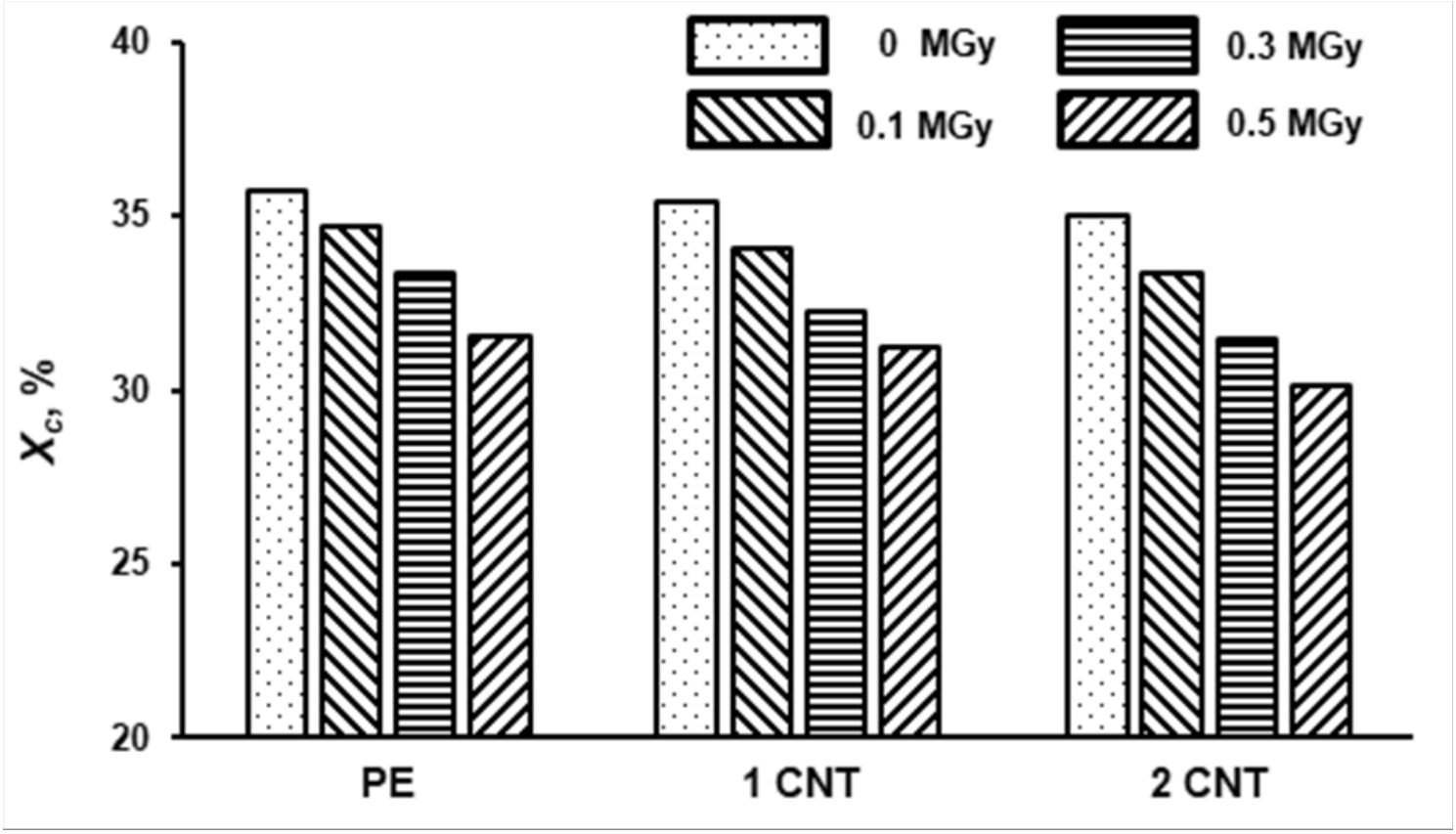

Figure 2

Degree of crystallinity of PE and its composites at different absorbed radiation doses.

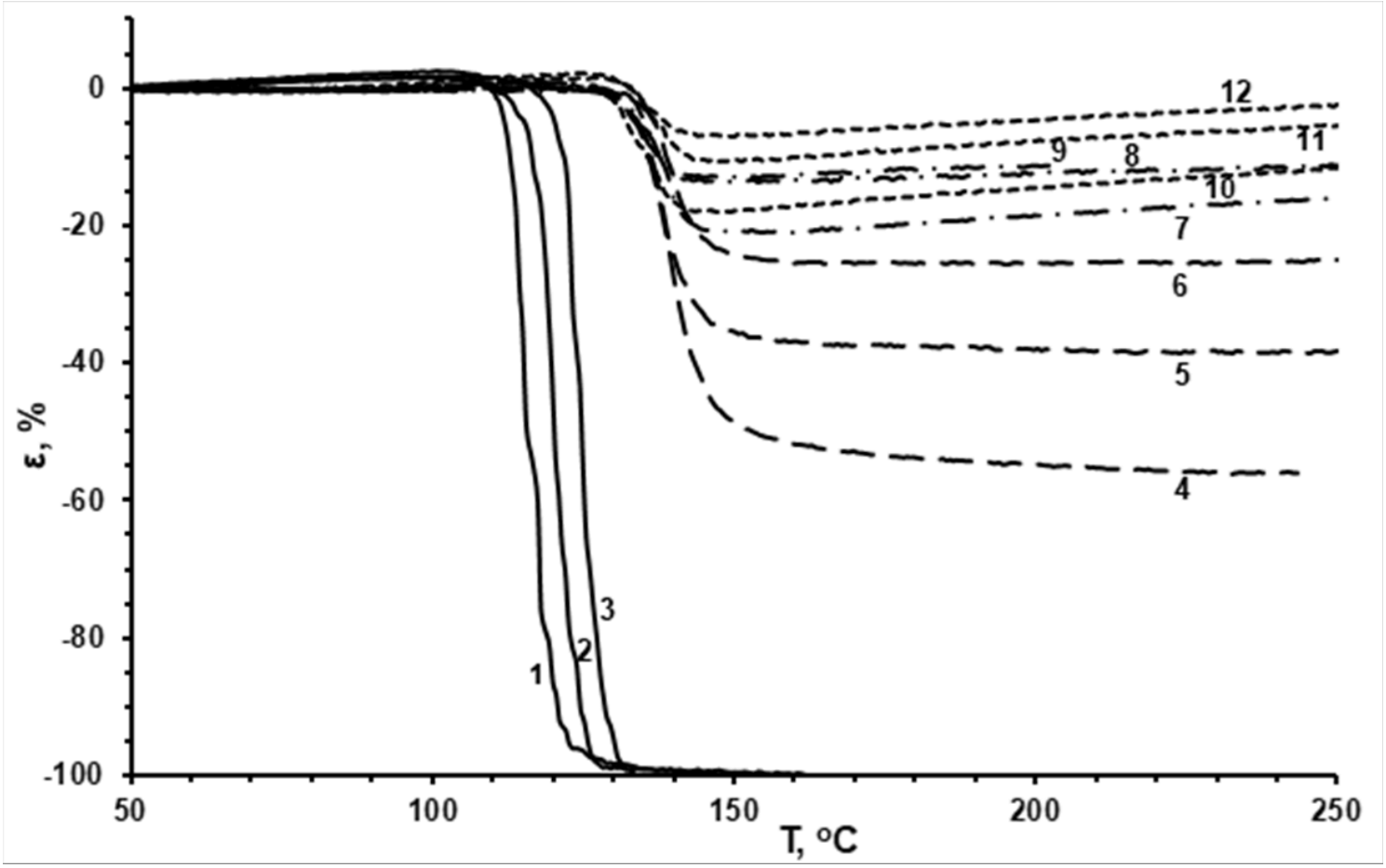

Figure 3

Temperature dependence of PE deformation and composites based on it. Curves: 1, 2, 3 - absorbed dose - 0 MGy; 4, 5, 6 - absorbed dose – 0.1 MGy; 7, 8, 9 - absorbed dose – 0.3 MGy; 10, 11, 12 - absorbed dose – 0.5 MGy. Curves 1, 4, 7, 10 - PE; 2, 5, 8, 11 - PE-1.0 vol.% MWCNT; 3, 6, 9, 12 - PE-2.0 vol.% MWCNT.

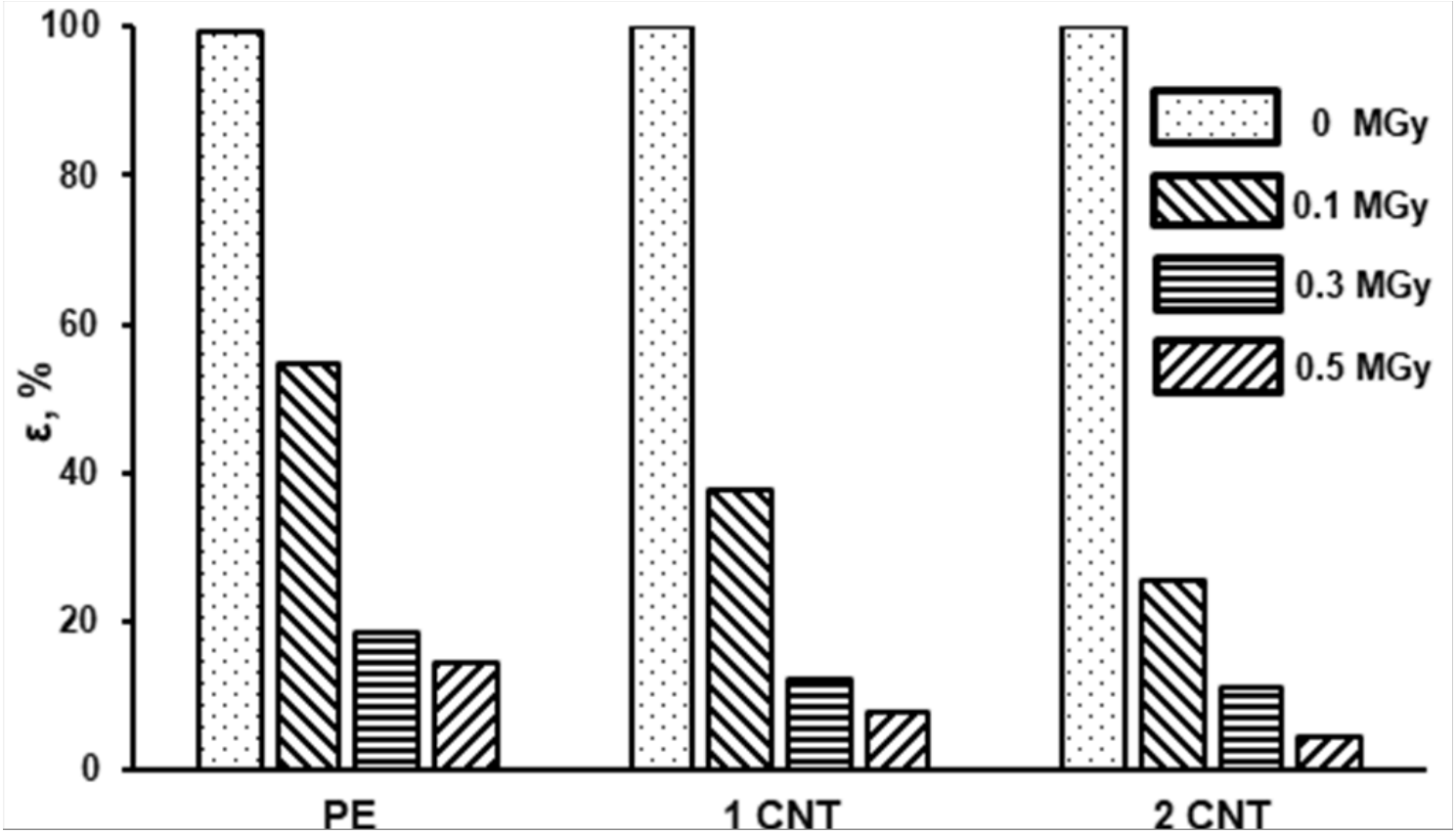

Figure 4

Deformation of PE and PE-MWCNT composites at a temperature of 200 °C at different absorbed doses of irradiation.

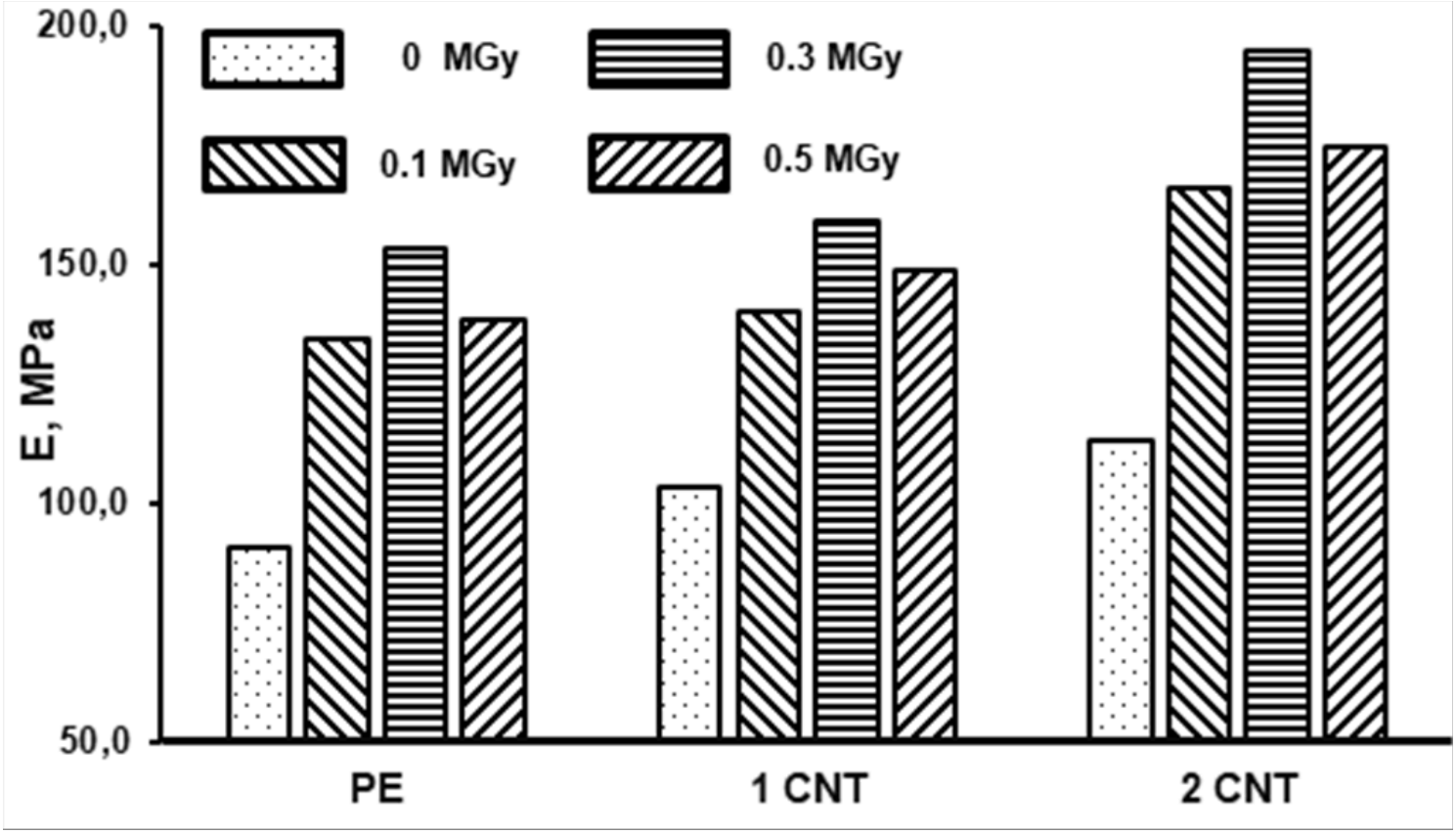

Figure 5

Modulus of elasticity of unfilled PE and its composites with 1.0 vol.% and 2.0 vol.% of MWCNT irradiated with different absorbed doses.

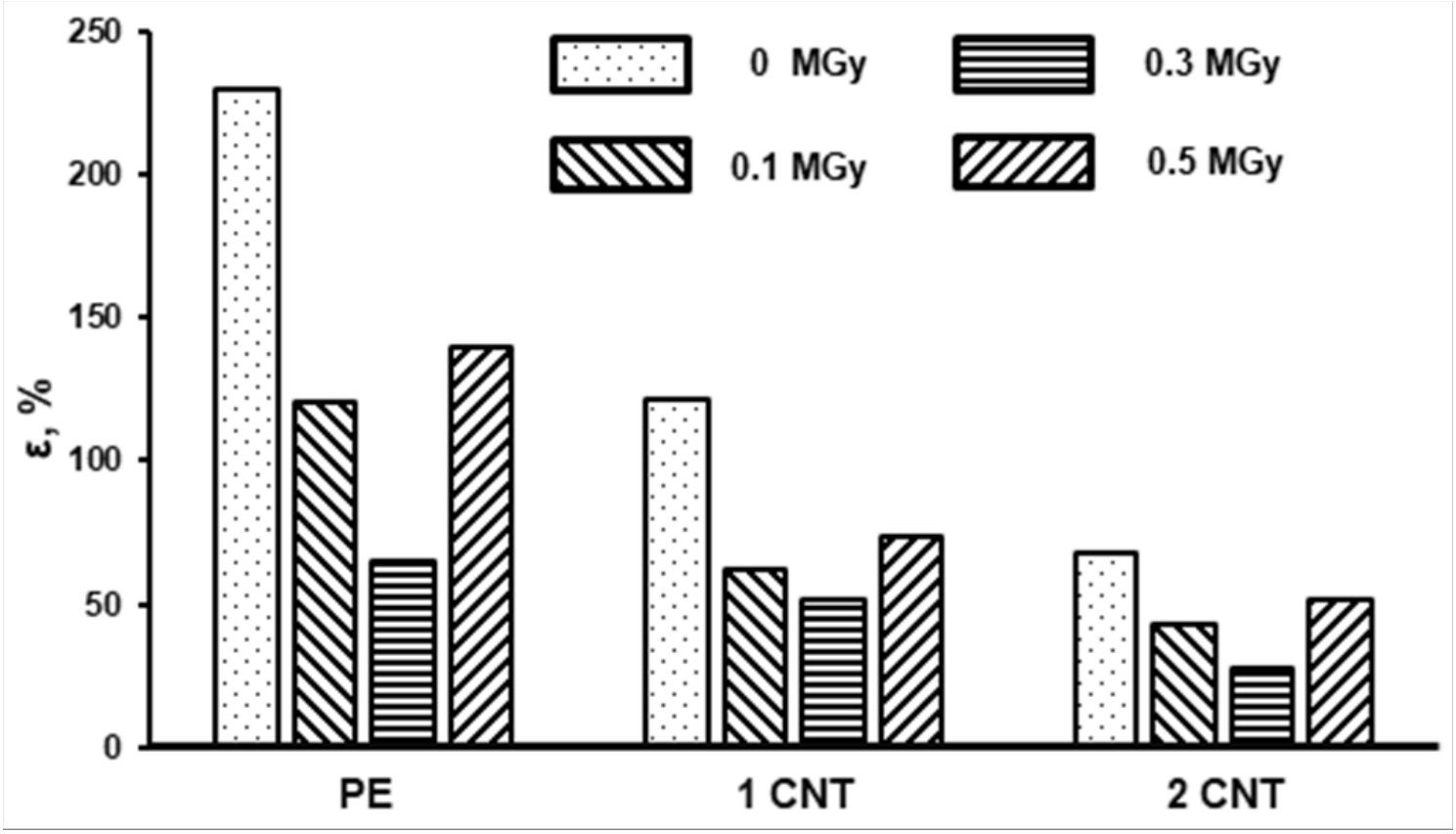

Figure 6

Deformation at break of PE and PE-MWCNT composites at different absorbed doses under irradiation.

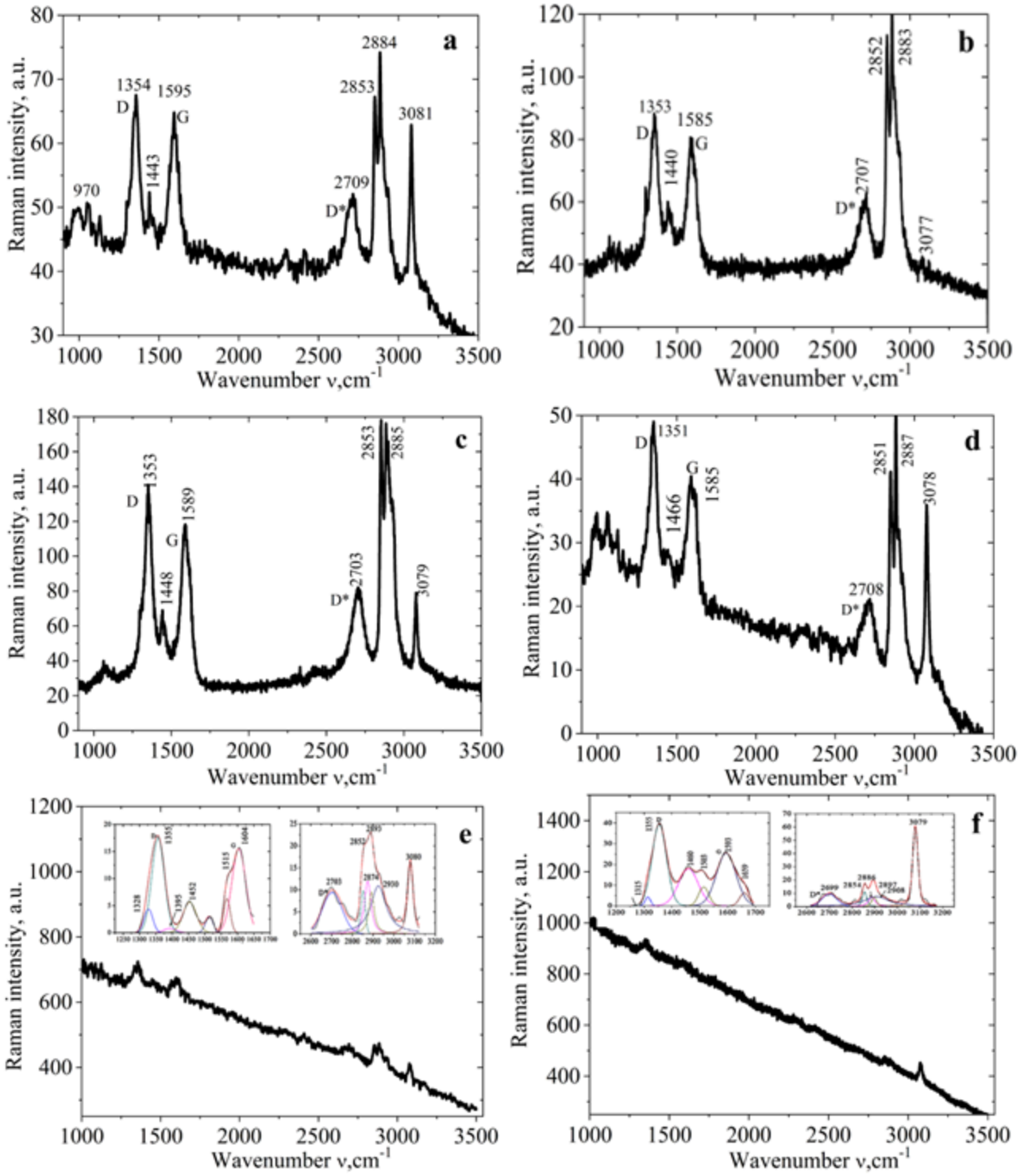

Figure 7

Raman spectra of polyethylene nanocomposites filled with 1.0 vol.% MWCNT in an unirradiated state (a) and after electron irradiation with absorbed doses of 0.05 (b), 0.2 (c), 0.7 (d), 2.0 (e) and 4.72 MGy (f). (λ_{ex}=514.5 nm, T=293 K, E_e=1.8 MeV).

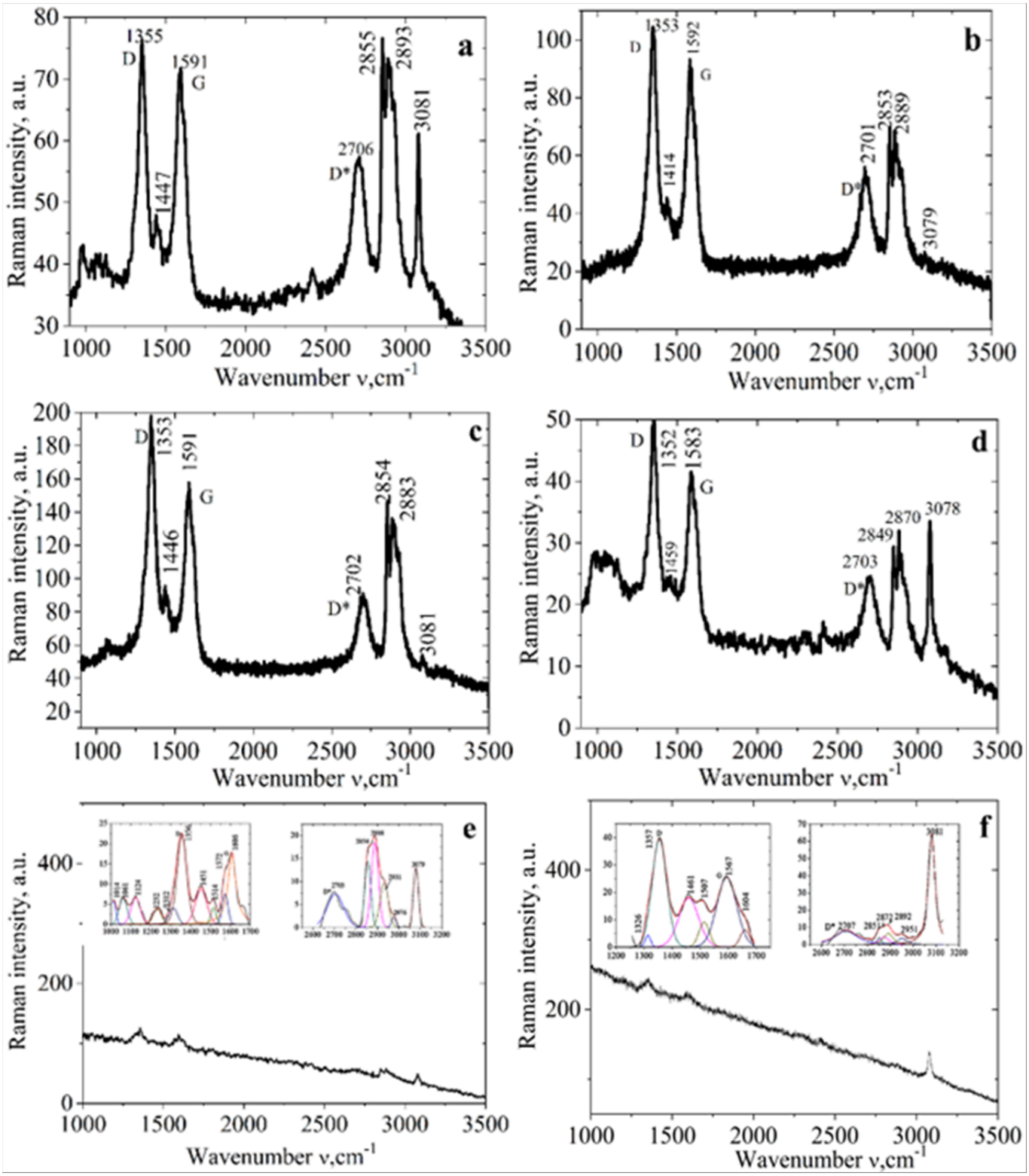

Figure 8

Raman spectra of polyethylene nanocomposites filled with 2.0 vol.% MWCNT in an unirradiated state (a) and after electron irradiation with absorbed doses of 0.05 (b), 0.2 (c), 0.7 (d), 2.0 (e) and 4.72 MGy (f) (λ_{ex}=514.5 nm, T=293 K, E_e=1.8 MeV).

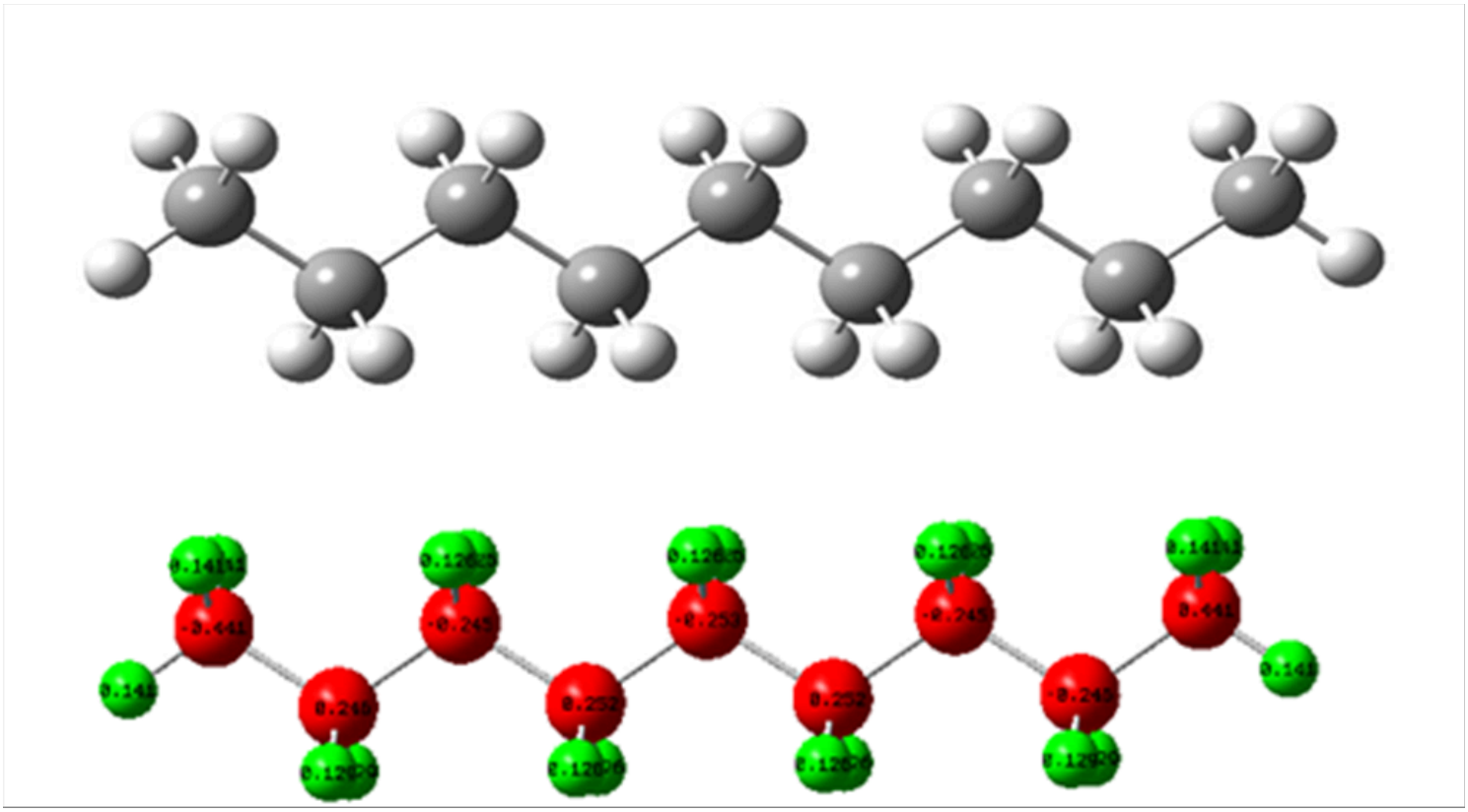

Figure 9

Optimised geometry (a) and charge distribution (b) of the C_9H_{20} polyethylene molecule.

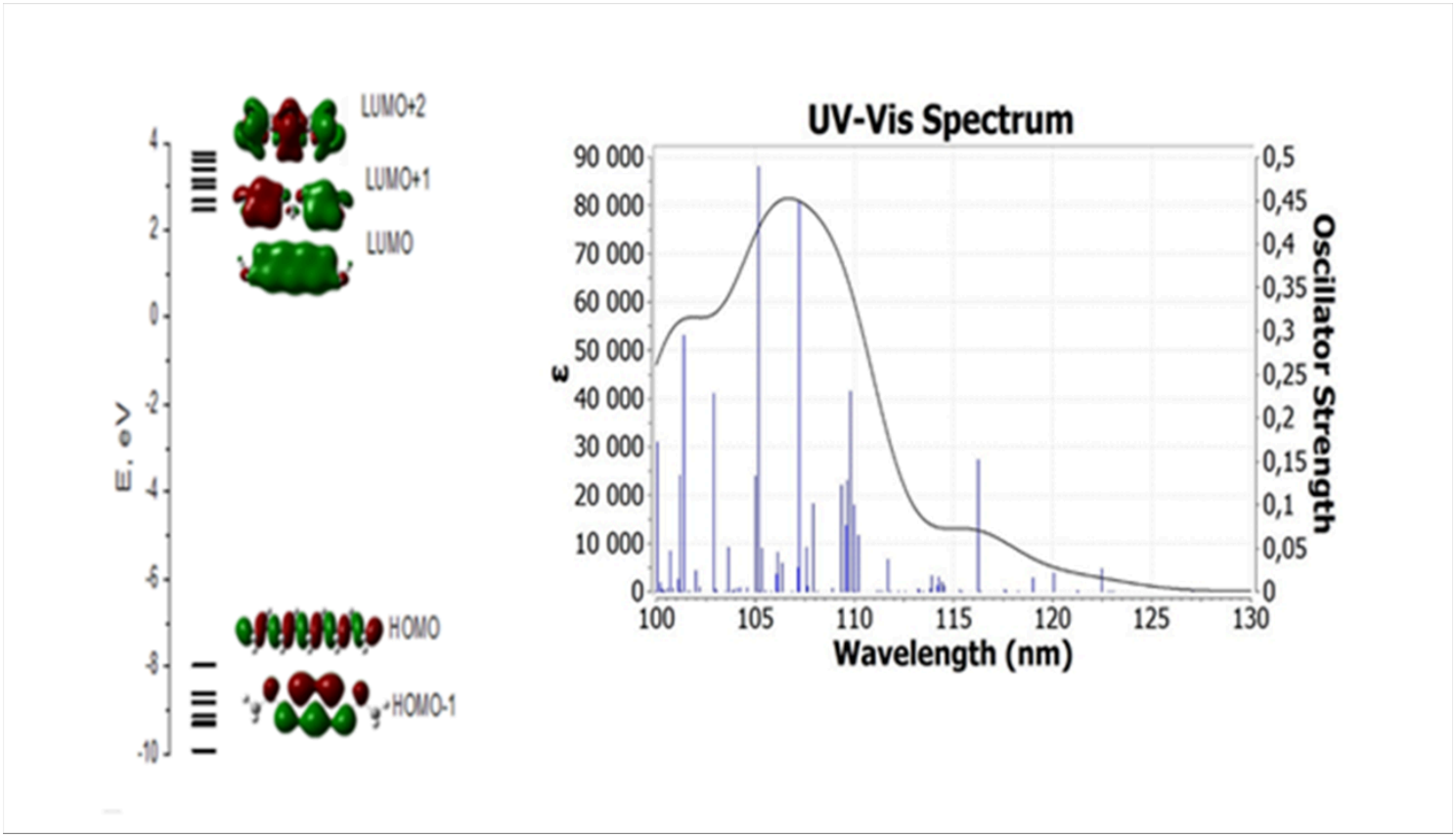

Figure 10

Distribution of electronic levels and molecular orbital shapes within the energy gap region, and the calculated absorption spectrum of the PE link.

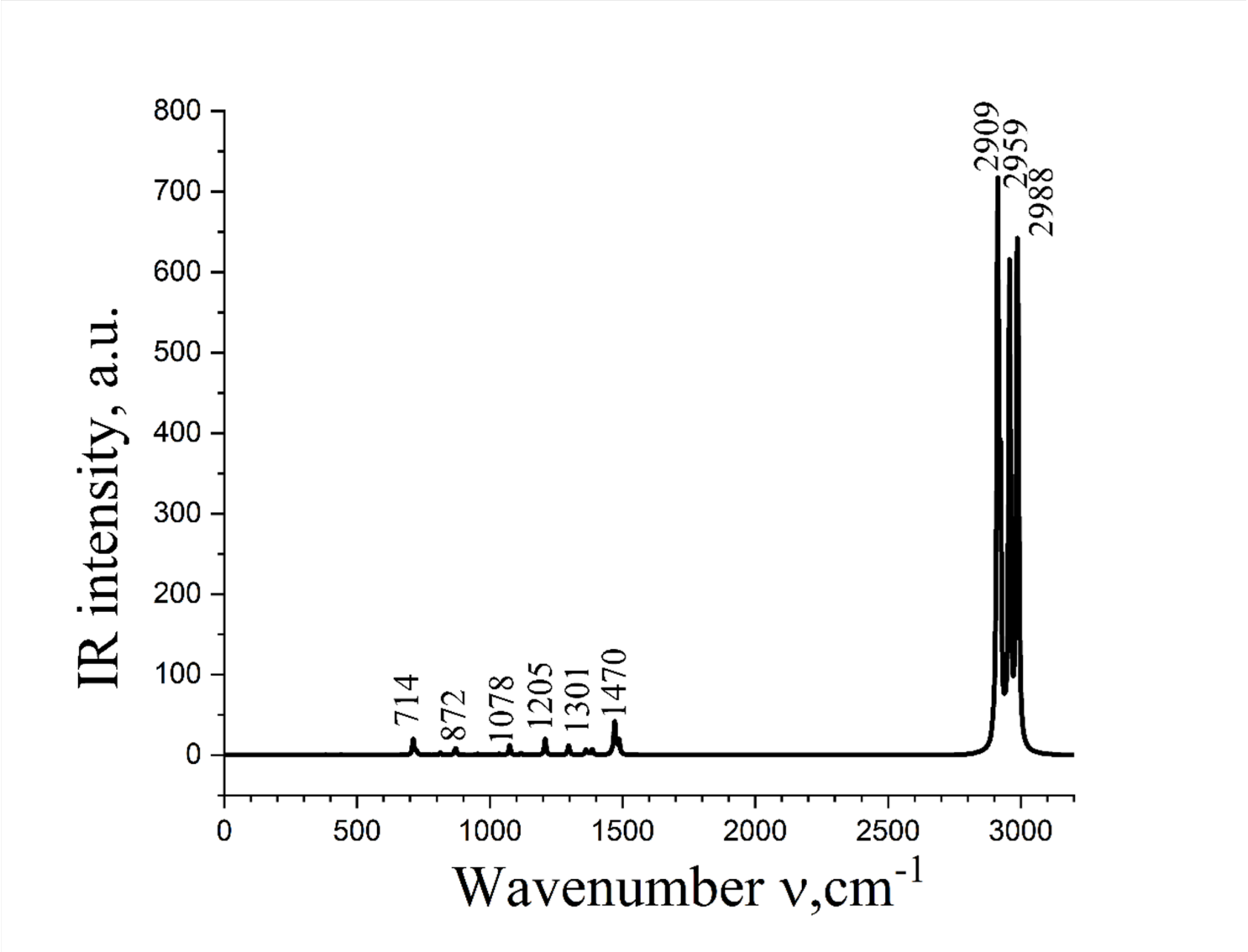

Figure 11

Calculated IR absorption spectrum of the polyethylene molecule C9H20 (scale factor 0.9614).

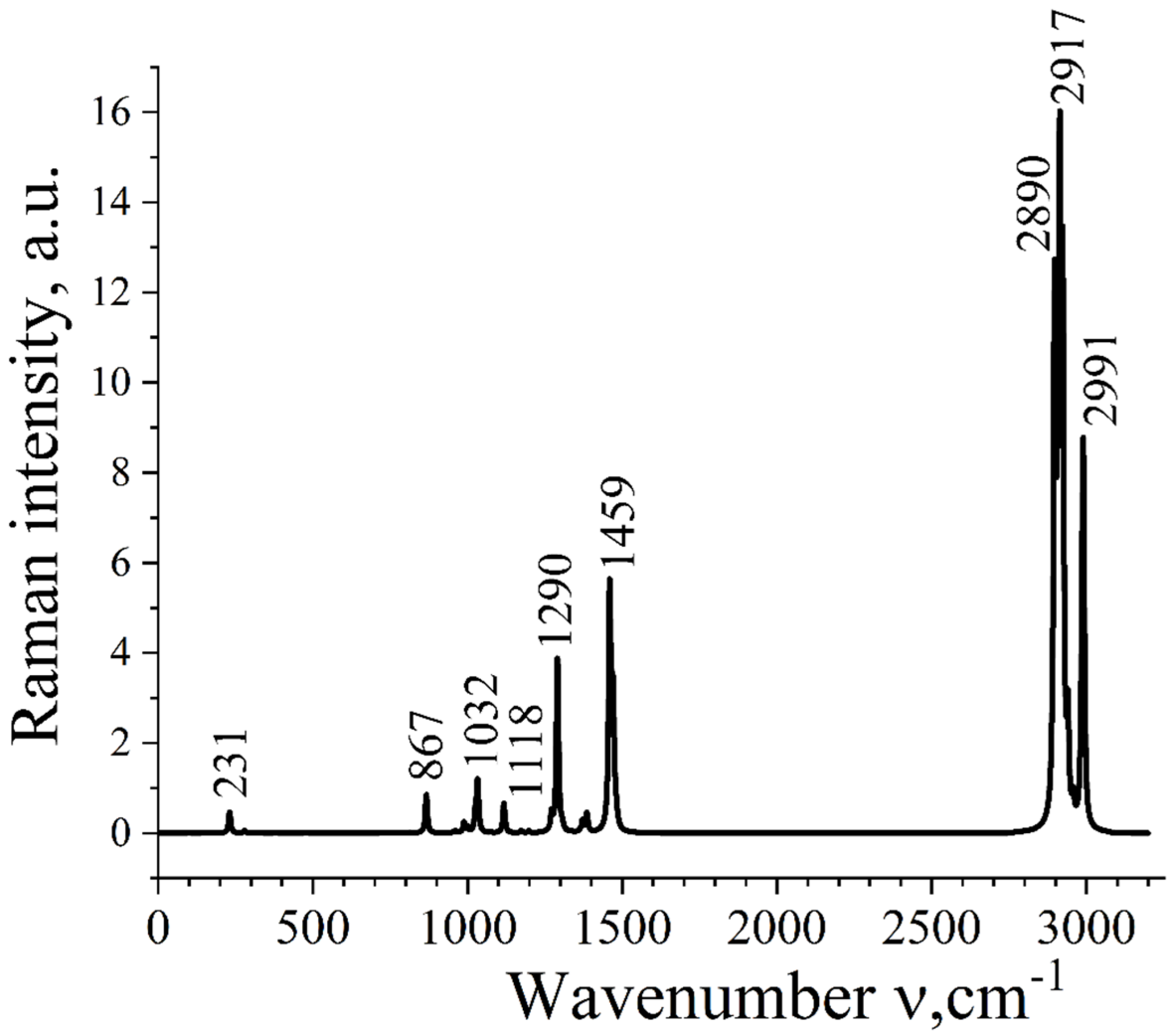

Figure 12

Calculated Raman spectrum of the C_9H_{20} molecule (scale factor 0.9614).